Supernova Relic Neutrino Search Results from Super-Kamiokande

Matthew Malek [1]
for the Super-Kamiokande collaboration
(1) Department of Physics and Astronomy, State University of New York, Stony Brook, NY 11794-3800, USA

Abstract

A search for relic neutrinos from all past core-collapse supernovae was conducted using 1496 days of data from the Super-Kamiokande detector. This analysis looked for $\bar{\nu}_e$ that had produced a positron with an energy greater than 18 MeV. In the absence of a signal, 90% C.L. upper limits on the total flux were set for several theoretical models. Additionally, an model-insensitive upper bound was set for the supernova relic neutrino flux in the energy region $E_\nu > 19.3$ MeV.

1. Introduction

During a core-collapse supernova, approximately 10^{53} ergs of energy are released, about 99% of which are in the form of neutrinos. It is generally believed that there exists a diffuse background of neutrinos originating from all the supernovae that have ever occurred. Detection of these supernova relic neutrinos (SRN) would offer insight about the history of star formation.

All types of neutrinos are emitted from a core-collapse supernova, but not all are equally detectable. The $\bar{\nu}_e$ is most likely to be detected by Super-Kamiokande (SK). It interacts primarily through inverse β decay with a cross section that is two orders of magnitude greater than that of neutrino-electron elastic scattering. All further discussion herein of the SRN refers only to the $\bar{\nu}_e$.

In this paper, Super-Kamiokande search results are compared to SRN predictions from six theoretical models [1-6]. The flux predictions range from 2 – 54 cm^{-2} s^{-1}. Three predictions are derived from galaxy evolution models, one is based on observed heavy metal abundances, one assumes a constant supernova rate, and one includes the effects of large mixing angle (LMA) neutrino oscillation.

2. Data Reduction

This paper presents the results of a search for SRNs in the Super-Kamiokande (SK) detector. SK is a water Cherenkov detector, with a fiducial mass of 22.5 kton. The data reported here were collected between May

pp. 1289–1292

31, 1996, and July 15, 2001, yielding a livetime of 1496 days. Backgrounds to the SRN signal are solar neutrinos, atmospheric neutrinos, and muon-induced spallation products.

Spallation is the most serious background, and the ability to remove it determines the lower threshold of the SRN search. A likelihood function uses information about cosmic ray muons to identify and remove spallation events. Furthermore, all events that occur less than 0.15 s after a cosmic ray muon are rejected. The spallation cut is applied to all events reconstructed with E < 34 MeV. No discernible spallation events with energies above 18 MeV remain in the data after this cut and so 18 MeV was set as the lower analysis threshold.

The sub-event cut removes muons produced by atmospheric ν_μ via charged current quasi-elastic scattering ($\nu_\mu\ N \to \mu\ N'$). Muons with low energies will stop in SK and produce a decay electron; often the muon and decay electron are found in the same event. The decay electron is then referred to as a "sub-event." If more than one timing peak is present in an event, then the event was removed.

Most remaining muons are removed by the Cherenkov angle cut. This cut exploits the mass difference between the muon and the positron, which results in a difference in their Cherenkov angles θ_C; all particles with $\theta_C < 37°$ were removed from the data. The efficiency of this selection criterion for retaining signal is 98%. Applying the Cherenkov angle cut and the sub-event cut together results in the rejection of > 99% of the muon background. The Cherenkov angle cut was also used to remove events with $\theta_C > 50°$. This eliminated events without clear Cherenkov rings, such as multiple γ rays emitted during a nuclear de-excitation.

Finally, a cut on the direction of the event is made to remove contamination from solar neutrinos. Events with E < 34 MeV were removed if the reconstructed event direction pointed back to within thirty degrees of the Sun.

The efficiency of the full data reduction is $47 \pm 0.4\%$ for $E \leq 34$ MeV, and $79 \pm 0.5\%$ for $E > 34$ MeV. Figure 1a plots the energy spectrum after applying each cut to events at all energies; note that in the final data set, the spallation cut and the solar direction cut will only be applied to the first four energy bins.

3. Analysis and Results

After applying the selection criteria, two irreducible backgrounds remain. The first is atmospheric ν_e events. The second comes from atmospheric ν_μ that form a muon that is below the Cherenkov threshold. These muons are said to be invisible and their decay electrons are not tagged as background events.

The energy spectra of these backgrounds have shapes that are very different from each other and from the SRN signal shape. Therefore, a three parameter shape fit was used to search for the SRN. The data were divided into sixteen energy bins and the following χ^2 function was minimized with respect to α, β, and γ:

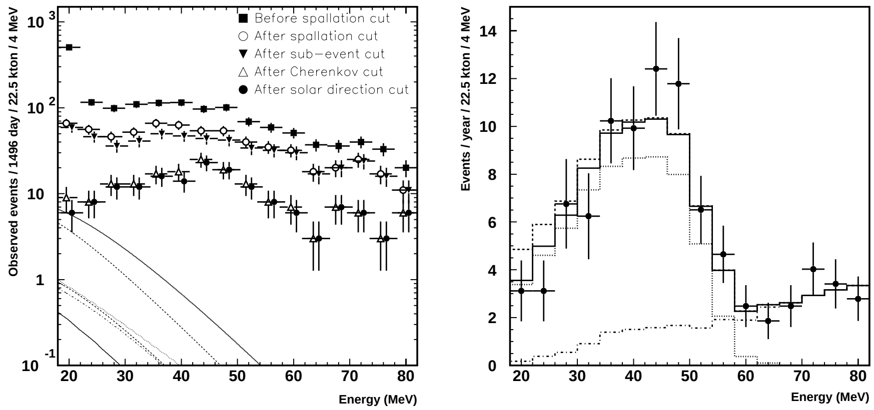

Fig. 1. The left figure (a) shows the energy spectrum at each reduction step, as well as the predictions from various theoretical SRN models. The right figure (b) shows the energy spectrum of SRN candidates. The dotted and dash-dot histograms are the fitted backgrounds from invisible muons and atmospheric ν_e. The solid histogram is the sum of these two backgrounds. The dashed line shows the sum of the total background and the 90% upper limit of the SRN signal.

$$\chi^2 = \sum_{l=1}^{16} \frac{[(\alpha \cdot A_l) + (\beta \cdot B_l) + (\gamma \cdot C_l) - N_l]^2}{\sigma_{stat}^2 + \sigma_{sys}^2} \tag{1}$$

In this equation, the sum l is over all energy bins and N_l is the number of events in the l^{th} bin. A_l, B_l, and C_l represent, respectively, the fractions of the SRN, Michel, and atmospheric ν_e spectra that are in the l^{th} bin.

The efficiency-corrected event rate spectrum of SRN candidates and the results of the fit are displayed in Figure 1b, which shows that the expected backgrounds fit the data well. For all six models, the best fit to α was zero and the minimum χ^2 value was 8.1 for 13 degrees of freedom. Thus, a 90% C.L. limit on α was set for each model and used to derive a 90% C.L. limit on the SRN flux from each model. The number of SRN events is related to the total flux F by:

$$F = \frac{\alpha}{N_p \times \tau \int_{19.3\,\mathrm{MeV}}^{\infty} f(E_\nu)\sigma(E_\nu)\epsilon(E_\nu)dE_\nu} \tag{2}$$

In this equation, N_p is the number of free protons in SK (1.5×10^{33}), τ is the detector livetime (1496 days), $\epsilon(E)$ is the signal detection efficiency, $\sigma(E)$ is the cross section for the inverse β decay (9.52×10^{-44} $\mathrm{E_e}$ $\mathrm{p_e}$), and $f(E)$ is the normalized SRN spectrum shape. The integral spans the energy range of the neutrinos that produce positrons in the observed region.

The SRN limits (see Table 1) vary greatly, based on the shape of the

Table 1. The SRN search results are presented for six theoretical models.

Theoretical model	Event rate limit (90% C.L.)	SRN flux limit (90% C.L.)	Predicted flux
Population Synthesis [6]	< 3.2 events/year	$< 130\ \bar{\nu}_e$ cm^{-2} s^{-1}	$44\ \bar{\nu}_e$ cm^{-2} s^{-1}
Cosmic gas infall [4]	< 2.8 events/year	$< 32\ \bar{\nu}_e$ cm^{-2} s^{-1}	$5.4\ \bar{\nu}_e$ cm^{-2} s^{-1}
Cosmic chemical evolution [2]	< 3.3 events/year	$< 25\ \bar{\nu}_e$ cm^{-2} s^{-1}	$8.3\ \bar{\nu}_e$ cm^{-2} s^{-1}
Heavy metal abundance [3]	< 3.0 events/year	$< 29\ \bar{\nu}_e$ cm^{-2} s^{-1}	$< 54\ \bar{\nu}_e$ cm^{-2} s^{-1}
Constant supernova rate [5]	< 3.4 events/year	$< 20\ \bar{\nu}_e$ cm^{-2} s^{-1}	$52\ \bar{\nu}_e$ cm^{-2} s^{-1}
Large mixing angle osc. [1]	< 3.5 events/year	$< 31\ \bar{\nu}_e$ cm^{-2} s^{-1}	$11\ \bar{\nu}_e$ cm^{-2} s^{-1}

theoretical SRN spectrum at energies that are below SK's SRN analysis threshold. To remove this strong model dependence, a limit was set for $E_\nu > 19.3\,\mathrm{MeV}$. In this region, all six models have similar energy spectrum shapes, and so an experimental limit that is insensitive to the choice of model can be obtained:

$$F_{ins} = F \times \frac{\int_{19.3\,\mathrm{MeV}}^{\infty} f(E_\nu)dE_\nu}{\int_0^{\infty} f(E_\nu)dE_\nu} \tag{3}$$

Flux limits in this energy region were the same for all models considered: $1.2\ \bar{\nu}_e$ cm^{-2} s^{-1}. Previously, the best limit on the SRN flux in this region was $226\ \bar{\nu}_e$ cm^{-2} s^{-1} [7]; the current SK limit is two orders of magnitude lower.

4. Conclusions

A search for the diffuse $\bar{\nu}_e$ from all previous core-collapse supernovae was conducted. No appreciable signal was detected in 1496 days of SK data. SRN flux limits were set for various models and a model-insensitive limit of $1.2\ \bar{\nu}_e$ cm^{-2} s^{-1} was set above a threshold of $E_\nu > 19.3$ MeV. These results are more than an order of magnitude better than previous limits; some theories regarding the supernova rate in the universe can be constrained or rejected by these limits.

5. References

1. S. Ando, K. Sato, and T. Totani, Astropart. Phys. 18, 307 (2003).
2. D. H. Hartmann and S. E. Woosley, Astropart. Phys. **7**, 137 (1997).
3. M. Kaplinghat *et al.*, Phys. Rev. D **62**, 043001 (2000).
4. R. A. Malaney, Astropart. Phys. **7**, 125 (1997).
5. T. Totani and K. Sato, Astropart. Phys. **3**, 367 (1995).
6. T. Totani, K. Sato, and Y. Yoshii, Astrophys. J. **460**, 303 (1996).
7. W. Zhang *et al.*, Phys. Rev. Lett. **61**, 385 (1988)